EDAXinsight

July 2015

Volume 13 Issue 2

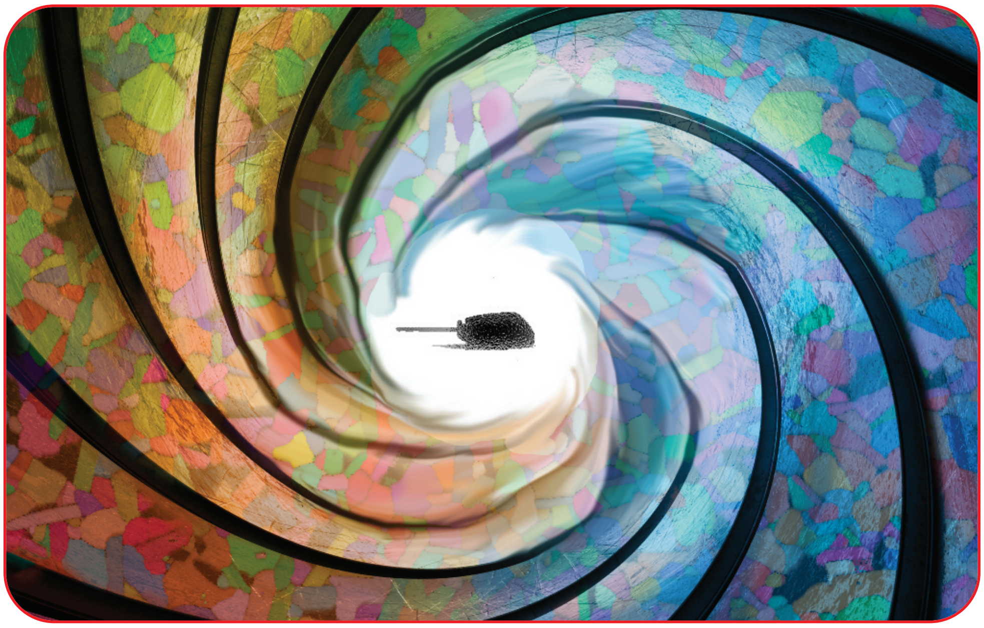

EDAX NEWS

Octane Elite SDD Series Lowers the (Analysis)Bar with New Silicon Nitride Windows

Scanning Electron Microscopes (SEMs) have made significant advances in the last decade, especially in the areas of signal detection and low voltage performance. The low voltage improvements are of special interest to the world of materials characterization because the decreased accelerating voltage leads to smaller interaction volumes and allows analysis of smaller features and thinner films in today's nano-world. Figure 1 shows the dramatic effect of kV on the true analysis region of a sample.

As critical features of samples move to smaller and smaller dimensions, analytical tools need to evolve to be able to meet the market requirements.

The new EDAX Octane Elite Silicon Drift Detector (SDD) Series of Energy Dispersive Spectroscopy (EDS) systems has taken a huge step in this direction with the introduction of silicon nitride entry windows, replacing the polymer windows that have been standard since the inception of SDD technology.

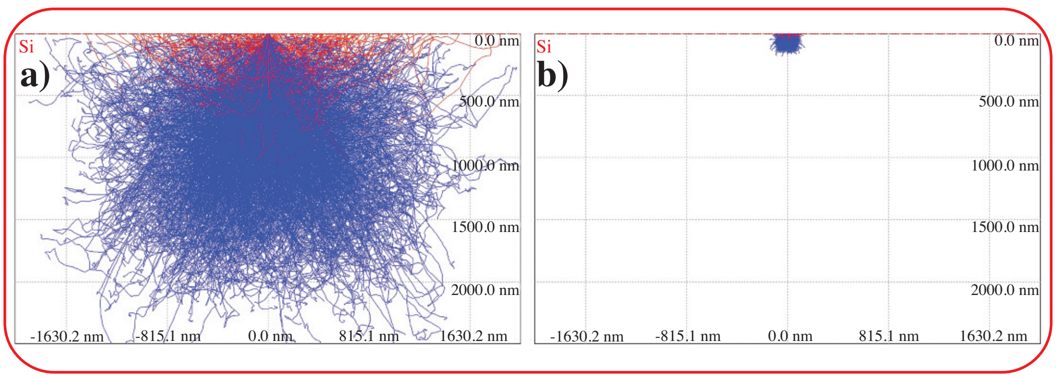

Figure 1. Monte Carlo simulation showing electron trajectories in silicon at (a) 15 kV and (b) 3 kV.

(Continued from Page 1)

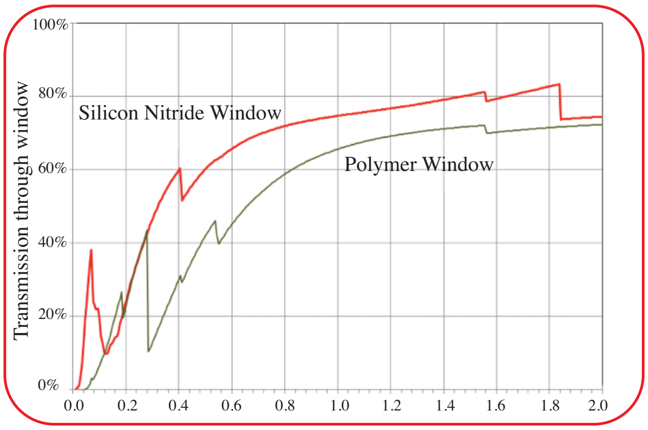

Figure 2. Silicon nitride windows offer increased transmissivity compared to polymer windows.

Silicon nitride (Si_3N_4) is a very durable material, known for thermal, corrosion and shock resistance, and it is chemically inert, except to HF, H_2SO_4 and other strong acids in presence of humidity and high temperatures above 140°C[1]. Si_3N_4 is often used in cutting tool applications due to its fracture toughness, hardness and wear resistance, and additionally, it is often the material of choice for passivation barriers in microelectronics. While this durability is a benefit for EDS applications, and provides more robust and reliable detectors, the true benefits of silicon nitride for EDS applications lie elsewhere.

Si_3N_4 properties allow the windows to be very thinly fabricated, which offers tremendous benefits in terms of sensitivity to soft X-rays, as required for optimal low voltage analysis. Figure 2 shows the X-ray transmission of a silicon nitride window compared to a polymer window, for a wide range of X-ray energies.

The transmission improvements of the silicon nitride window can be as much as 35% compared to the polymer window, leading to greatly improved light element performance and significantly more critical data

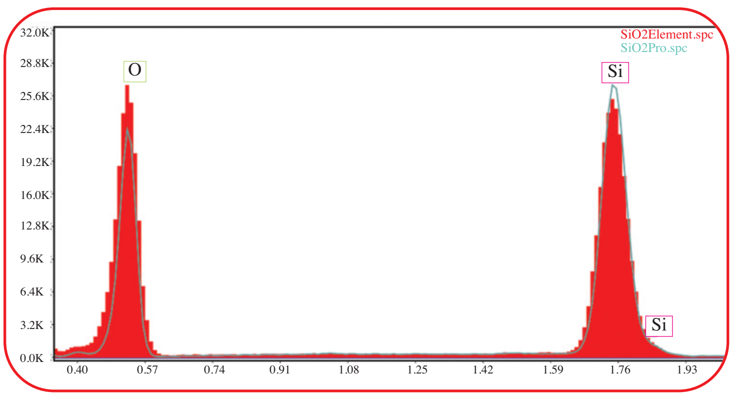

Figure 3. Shows the spectra acquired from a silicon dioxide sample at 10 kV. The two spectra have been scaled to the same peak amplitude at the Si K peak to facilitate comparison and a clear improvement for the silicon nitride window is seen in the increased oxygen peak intensity.

for the materials analyst (Figure 3). Additionally, the mechanical properties of the silicon nitride allow for a reduction in the area of the necessary support grid, compared to the polymer window, offering further efficiencies and another increase in real world throughput and data collection.

The spectra in Figure 4 show the outstanding low energy performance of the silicon nitride window for low energy X-rays. Using low kV to analyze a beam sensitive material like Teflon accurately identifies the elements present and their peak intensities.

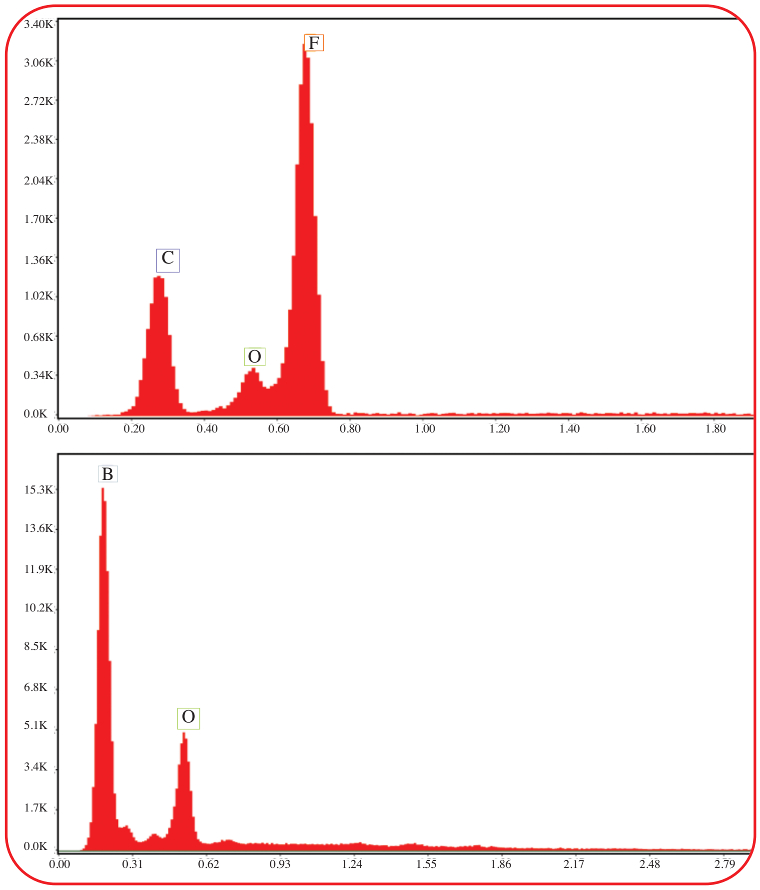

Figure 4. Shows an example of very low element sensitivity, Teflon (above), which contains carbon, oxygen and fluorine, and a boron containing sample (below). The spectra were acquired at 5 kV. The intensity of the peaks is a function of the increased transmission of the low energy X-rays through the silicon nitride window.

This window will be a great advantage, paired with the low voltage performance of moderns SEMs, for materials analysts trying to meet the extreme challenges of nano-analysis involved in today's characterization problems. The EDAX Octane Elite SDD Series with silicon nitride windows puts EDAX customers on the cutting edge of microanalysis and allows them to solve their most difficult analysis challenges.

[1] *http://accuratus.com/silinit.html*

Which XRF Line Series to Use?

The direct analysis range of benchtop Energy Dispersive X-ray Fluorescence (ED-XRF) Analyzers using 50 kV X-ray tubes generally runs from Na to Bk. Portions of this elemental range generate two sets of X-ray line series, which can be measured and used for analysis. These nominal elemental ranges are Zn to Ba generating L and K series and Nd to Bk generating M and L series. The question often comes up as to which line series is the best to use and the answer is always, "It depends on the situation". One should consider a number of factors including line intensity (which includes excitation and detection efficiency), line overlaps and interferences, and matrix absorption effects.

In general, the higher energy lines are preferred. The number of possible electron transitions producing the X-ray signal is lower for the higher energy line series (i.e. K vs L), which means the Kα lines are more intense than the Lα lines and the potential for line overlap is lower for the higher energy K lines. This can often be a relatively simple exercise of comparing the line intensities and peak-to-background ratios to determine which X-ray line series provides the best precision without spectral overlaps.

There are certain times when the lower energy line series can be more useful. For example, when measuring the thickness of thin metallic coating layers, where "thin" is characterized by the signal absorption of the layer being measured versus the energy of the X-ray signal, the lower energy line series is more sensitive to change in layer thickness. Hence, a small change in "thin" layer thickness evokes a greater change in lower energy signal intensity compared to the higher energy line series. However, the lower energy line series will obviously saturate at a lower thickness limit than the higher energy line series.

The analysis of more complicated sample structures is another instance where one should also consider the use of the lower energy line series. In one case, a customer wanted to measure the Sn coating thickness on an electrical component. Results using the Sn(L) and Sn(K) lines were not similar (Table 1) even when the quantitative models were calibrated with the same type standard. The reason was that the sample component was coated on both sides of the substrate and the substrate was an Al alloy about 0.8 mm thick. The substrate could only absorb about 30% of the Sn(K) fluorescence generated from the opposing surface while it would absorb essentially 100% of the Sn(L) fluorescence. Once the coating was removed from one side of the electrical component to test this hypothesis, the Sn(L) and Sn(K) measurements fell into the same range (Table 2). The measurement of the underlying Ni-alloy layer thickness was now consistent because the result of the Ni thickness, which had the same Ni signal intensity in either case, depended on the calculated value of the Sn layer above it.

There is a website (http://henke.lbl.gov/optical_constants/filter2.html) that calculates the absorption characteristics of a sample matrix, which can be used to verify the probe depth of XRF. The probe depth depends on the matrix absorption characteristics, as well as the X-ray signal line energy.

This website calculator can accept input of multi-element sample matrix formulae and density (it also calculates theoretical density in lieu of manual input) and outputs transmission/absorption characteristics from 1 to 30 keV with a resolution of up to 500 intervals.

Sn(L) on Ni(ZnCu) on Al base					**Sn(K) on Ni(ZnCu) on Al base**			
Layer	Element	Thickness (μm)	Composition (wt%)	Measurement Position	Layer	Element	Thickness (μm)	Composition (wt%)
1	Sn	1.44	100.0	Eyelet Side	1	Sn	2.52	100.0
2	Ni	1.26	86.9		2	Ni	1.98	87.5
2	Cu		2.2		2	Cu		2.1
2	Zn		10.9		2	Zn		10.4
Base	Al		99.7		Base	Al		99.7
	Fe		0.3			Fe		0.3

Table 1. Initial coating thickness measurements on the electrical contact surface comparing measurements made with Sn(L) and Sn(K) lines.

Sn(L) on Ni(ZnCu) on Al base					**Sn(K) on Ni(ZnCu) on Al base**			
Layer	Element	Thickness (μm)	Composition (wt%)	Measurement Position	Layer	Element	Thickness (μm)	Composition (wt%)
1	Sn	1.58	100.0	Eyelet Side	1	Sn	1.47	100.0
2	Ni	1.27	86.7		2	Ni	1.21	86.6
2	Cu		2.2		2	Cu		2.2
2	Zn		11.1		2	Zn		11.2
Base	Al		99.7		Base	Al		99.7
	Fe		0.3			Fe		0.3

Table 2. Comparison of coating measurements using Sn(L) and Sn(K) after coating on the opposing side of the electrical contact was removed by polishing.

APPLICATION NOTE

Fast Simultaneous EDS-EBSD Mapping and Chi-Scan Analysis

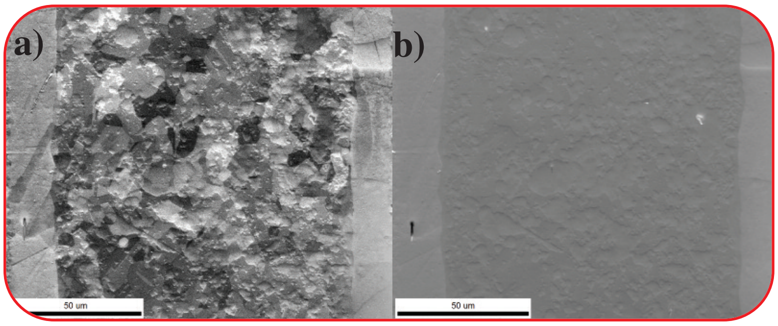

Figure 1. PRIAS (a) orientation contrast derived from the center square signal using PRIAS Collection and (b) phase contrast using the top strip signal.

In EDAX Insight Volume 12 Issue 4, fast acquisition of high quality Electron Backscatter Diffraction (EBSD) data was demonstrated with the Hikari Super EBSD Camera Series and TEAM™ Analysis software. Building upon this work, the goal of this article is to show that useful EDS compositional data can be collected simultaneously with EBSD orientation data at high speeds, where time of collection is a primary concern. This can be achieved by coupling Octane SDDs and a Hikari Super EBSD Camera, using the TEAM™ Pegasus Analysis System software.

Consider the material shown in Figure 1. These Pattern Region of Interest Analysis System (PRIAS) images show orientation contrast (Figure 1a) derived from the center square signal using PRIAS Collection functionality and phase contrast (Figure 1b) using the top strip signal. They reveal that the inner phase has a smaller average grain size than the outer coatings. The goal of this analysis is to accurately differentiate the phases so that the quantitative grain size and texture can be calculated and compared to understand the deposition and coating processes.

Simultaneous EDS-EBSD data was collected from the area of interest at 1,400 indexed points per second using the Hikari Super EBSD Camera and an Octane Super SDD. The Scanning Electron Microscope (SEM) operating conditions were 20 kV acceleration voltage and approximately 10 nA incident beam current. At these conditions, the input count rate on the EDS detector was approximately 464 kcps, with an output count rate of 267 kcps at a deadtime of 42%. These numbers show the high throughput capability of the Octane detectors.

Simultaneously collected EDS maps from iron (53 max counts), nickel (29 max counts), and copper (44 max counts) are shown in Figure 2. The center phase is a Fe-Ni alloy surrounded by a copper phase coating on each side. Obviously, the EDS information acquired at these speeds is sufficient to determine the phase distribution. However, both of these phases have a face-centered cubic crystal structure with similar lattice parameters (≈ 1% difference). With such similar structures, it is difficult for EBSD to reliably differentiate between these two phases, as shown in Figure 3. This image shows an EBSD phase map, with the Fe-Ni phase colored red and the copper phase colored blue. This image highlights the difficulty of differentiating similar crystallographic phases at high collection speeds.

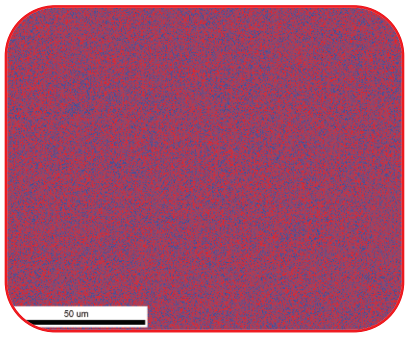

Figure 3. An EBSD phase map, with the Fe-Ni phase colored red and the copper phase colored blue. Phase differentiation is noisy due to similar FCC phases.

With simultaneously collected EBSD and EDS data, Chi-Scan can be used to differentiate the phases using EDS compositional information, while concurrently determining the crystallographic orientation using EBSD. Chi-Scan is a patented approach to analyzing simultaneous data for improving phase differentiation, using either patterns saved during EBSD collection or the stored position of the detected bands.

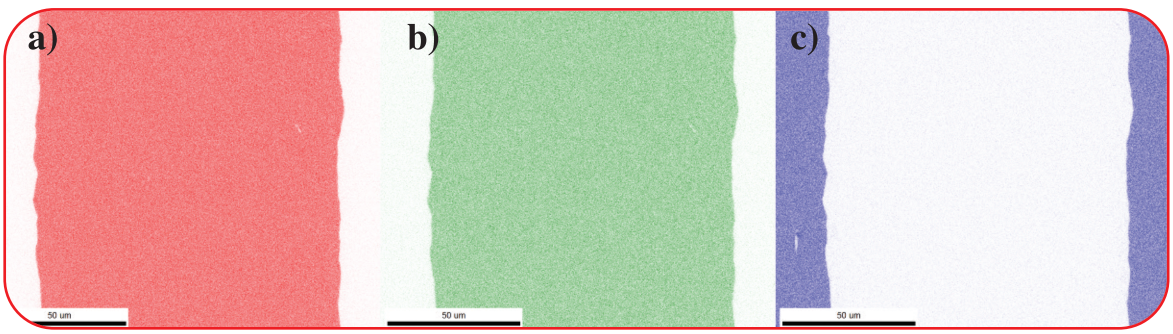

Figure 2. Simultaneously collected EDS maps from (a) iron (53 max counts), (b) nickel (29 max counts), and (c) copper (44 max counts). The center phase is a Fe-Ni alloy surrounded by a copper phase coating on each side.

(Continued from Page 4)

Figure 4. Phase map after Chi-Scan analysis.

Using the patterns saved during EBSD collection approach, band detection parameters via the Hough transform can be adjusted, while reprocessing times are faster utilizing the stored position of the detected bands approach. The phase map after Chi-Scan analysis is shown in Figure 4. Clearly, accurate phase differentiation has been achieved, matching the EDS and PRIAS information. The orientation map in Figure 5, shows that we have characterized composition, phase, and orientation.

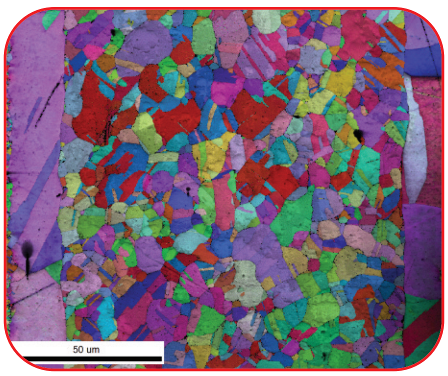

Figure 5. Orientation map showing characterized composition, phase, and orientation.

With this data, the partitioning functionality within Orientation Imaging Microscopy (OIM™) Analysis allows easy visualization of the grain size and structure for both the Fe-Ni phase (Figure 6a) and for the copper phase (Figure 6b). In these figures, the grains are randomly colored to show grain size and morphology, with no two adjacent grains having the same color. For this sample, the Fe-Ni phase has a normally distributed grain size, while the copper phase has a bi-modal grain size, with larger grains near the Fe-Ni phase interface and smaller grains away from it. The twin boundary fraction and preferred orientation of each phase can also be easily displayed.

This type of microstructural analysis of similar phases at high collection speeds is enabled by combining the high speed and high sensitivity of the Hikari Super EBSD Camera with the performance

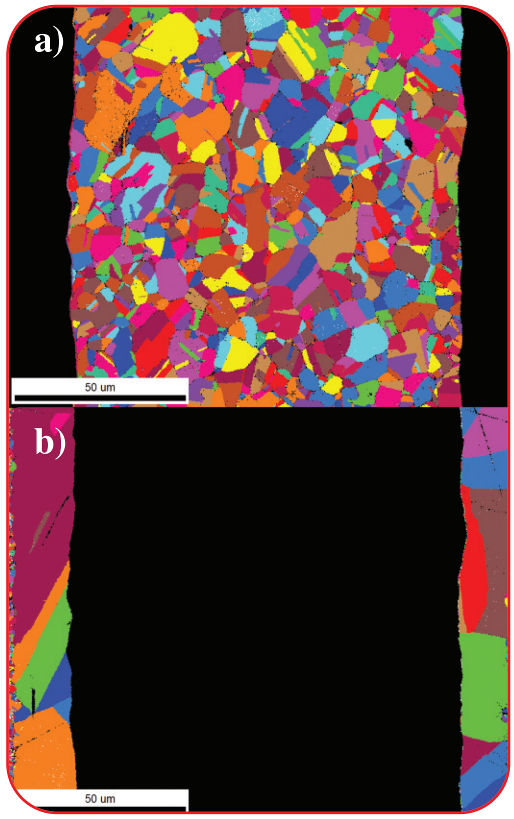

Figure 6. The partitioning functionality with OIM™ Analysis allows easy visualization of the grain size and structure for both the (a) Fe-Ni phase and (b) copper phase. The grains are randomly colored to show grain size and morphology, with no two adjacent grains having the same color.

and throughput capability of the Octane Super SDD and the indexing and processing capabilities of the TEAM™ Pegasus Analysis software. This capability is uniquely suited for in-situ characterization experiments, where time of collection is a primary concern.

References:

Nowell, M. M. and S. I. Wright (2004). "Phase differentiation via combined EBSD and XEDS." Journal of Microscopy 213(Pt 3): 296-305.

Wright, S. I., M. M. Nowell, R. de Kloe, P. Camus and T. Rampton (2015). "Electron imaging with an EBSD detector." Ultramicroscopy 148(0): 132-145.

Wright, S. I. and M. M. Nowell (2009). A Review of In Situ EBSD Studies Electron Backscatter Diffraction in Materials Science, 2nd Edition. A. J. Schwartz, M. Kumar, D. P. Field and B. L. Adams, Springer: 329-338.

EVENTS AND TRAINING

Worldwide Events

August 2-6
Microscopy & Microanalysis (M&M) 2015 — Portland, OR
August 3-7
Denver X-ray Conference — Westminster, CO
August 16-20
XXIV International Materials Research Congress (IMRC) — Cancun, Mexico
August 23-28
Multinational Congress on Microscopy (MCM) 2015 — Eger, Hungary
September 2-4
JASIS 2015 — Tokyo, Japan
September 6-11
Microscopy Conference (MC) 2015 — Göttingen, Germany
September 14-17
Werkstoffwoche 2015 — Dresden, Germany
September 16-18
Metallographie — Dresden, Germany

Please visit www.edax.com/Event/index.aspx for a complete list of our tradeshows.

2015 Worldwide Training

To help our present and potential customers obtain the most from their equipment and to increase their expertise in EDS microanalysis, WDS microanalysis, EBSD/OIM™ , and Micro-XRF systems, we organize a number of Operator Courses at the EDAX facilities in North America; Tilburg, NL; Wiesbaden, Germany; Japan, and China.

EUROPE

EDS Microanalysis	
TEAM™ EDS	
September 21-23	Tilburg*
November 16-18	Wiesbaden#
December 1-3	Wiesbaden#
December 8-10	Tilburg*
EBSD	
September 14-16	Tilburg*
November 18-20	Wiesbaden#
TEAM™ Pegasus (EDS & EBSD)	
November 16-20	Wiesbaden#
TEAM™ WDS	
September 23-25	Tilburg*
November 17-19	Tilburg*
TEAM™ Neptune (EDS & WDS)	
September 21-25	Tilburg*
XRF	
October 20-22	Tilburg*

*Presented in English
#Presented in German

JAPAN

EDS Microanalysis	
Genesis	
October 8-9	Tokyo
November 12-13	Osaka

CHINA

EDS Microanalysis	
TEAM™ EDS	
September 8-10	Shanghai (ACES)
TEAM™ EBSD OIM™ Academy	
October 20-22	Shanghai (ACES)
Particle Analysis	
December 8-10	Shanghai (ACES)

NORTH AMERICA

EDS Microanalysis	
TEAM™ EDS	
September 22-24	Mahwah, NJ
EBSD OIM™ Academy	
October 27-29	Draper, UT
Micro-XRF	
October 6-8	Mahwah, NJ

ONLINE

TEAM™ EBSD	
On Demand	3 Sessions

Please visit www.edax.com/support/training/index.aspx for a complete list and additional information on our training courses.

FOLLOW US

Stay up to date with news and happenings through social media.
Follow us on LinkedIn, Twitter, YouTube and at http://edaxblog.com.

Visit edax.com for the latest news and up-to-date product information.

EMPLOYEE SPOTLIGHT

Andreas Makat

Andreas Makat

Andreas started his career at EDAX in July of 1994. Based out of the Wiesbaden, Germany office, he is the senior strategic sales manager for the Europe, Middle East, and Africa (EMEA) regions. Andreas is responsible for coordinating EDAX's distributor network and all indirect sales channels within the EMEA region. He also handles direct sales in the northern part of Germany.

Prior to EDAX, Andreas worked for Vacuum Generators (VG Scienta), now VACGEN, in East Grinstead, United Kingdom, where he was the sales manager from 1987-1994. In 1987, Andreas earned his bachelor's degree in Mineralogy from Freie Universität Berlin. He also studied material sciences at the Technische Universität Berlin from 1978-1986.

Andreas and his wife Michaela have one daughter, Tabea Maria (nine). In his spare time, Andreas plays volleyball for a club team. He also likes to go bicycling and swimming with his family. Andreas tries to barbecue as often as possible.

(left to right): Shelby, Karen, Stephen, and Jessica Mann.

Stephen Mann

Stephen has worked at EDAX for 30 years. He joined the company in June 1985 as a technical support specialist in the Mahwah, NJ office. When EDAX moved the factory to New Jersey from Chicago, Stephen was assigned the service manager position and held that role until 2011. Since then, he has been working in the technical support department, providing direct technical support to EDAX customers, the company's field service engineers, and global associates.

Prior to EDAX, Stephen spent six years in the United States Navy working on attack bombers on shore and at sea on an aircraft carrier. Numerous Navy engineering schools and several deployments overseas prepared him for his career at EDAX. During that time, Stephen performed and supervised maintenance on aircraft electronic fire control systems and tactical displays with associated equipment.

Stephen lives with his wife, Karen, a special education teacher of 30 years. They have two children: Shelby (26), a police officer in Colorado and Jessica (21), who recently graduated from Mercy College of New York with a bachelor's degree in social science. In his off time, Stephen likes to work around his yard and gardens, play golf, softball, volleyball, and his favorite pastime is skiing.

2015 EDAX Webinars

For a complete list of all upcoming and on demand EDAX webinars, please visit: http://www.edax.com/webinars.

Low Energy and High Spatial Resolution EDS Mapping
In this webinar, we discuss the signal origin and limiting factors for the spatial resolution of the X-ray signal and see how we can optimize these parameters to achieve our data collection goals.

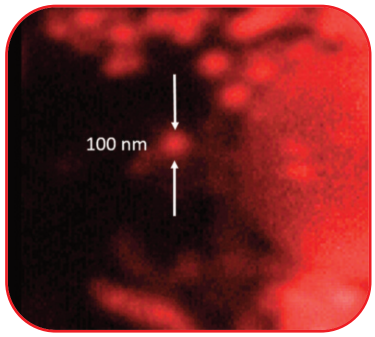

Smart SDD Technology with Quantitative Routines for Applied TEM Analysis
This webinar explains the specifications of the new Octane SDD Series for the Transmission Electron Microscope (TEM). We show how complex it is to determine the solid angle and to compare these numbers and demonstrate the quantification routine on TEMs based on the Cliff-Lorimer Method, which is used in our TEAM™ software. Finally, we give some application examples and show that spectral mapping with atomic resolution is now possible.

Using Small Spot XRF Analysis to Solve Industrial Forensic Challenges
In this event, the theory and strengths of XRF measurements are discussed followed by some examples from various industrial sectors.

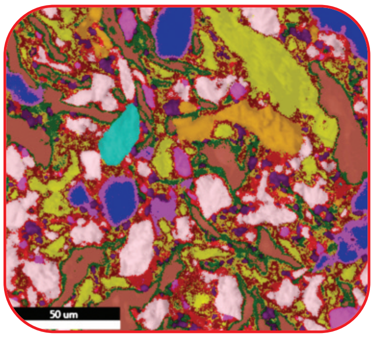

Spectrum Library Matching: Correlating Phase Map Spectra with Library Matching for Conclusive Solutions
In this webinar, we review some of the many applications of SML and how libraries can be customized according to sample types and industry needs. Using powerful data examples, we also explore the unique association between spectrum phase mapping and library matching for complete materials identification.

Modern XRF Solutions for Thin-Film Measurements and Process Control
This webinar discusses the capabilities of new analysis solutions in coating thickness and process control applications, and how they differ from current micro-XRF technology.

Maximizing the Use of PRIAS in TEAM™ and OIM™ Analysis: Applications from Materials, Microelectronics & Geologicals to Thin Foils
Pattern Region of Interest Analysis System (PRIAS) is a novel imaging tool, which utilizes market leading Electron Backscatter Diffraction (EBSD) hardware to visualize microstructure. It extracts several pieces of information from the backscattered electrons captured by the EBSD detector, including orientation contrast, chemistry contrast, topography, magnetic domains, and even thin film thickness variation.

This webinar explores how PRIAS images are formed in order to optimize collection parameters to achieve the best possible results. A number of different samples are presented which highlight the extent of PRIAS applications.

Past, present and future - the evolution of X-ray analysis
Energy Dispersive X-ray Microanalysis has a long history marked by major milestones in technology. These advancements have accelerated the capabilities towards analytical solutions for many fields of science. As the technology evolves, system performance reaches new levels and the number of applications continues to grow.

This webinar starts with an introduction to the underlying fundamentals of X-ray microanalysis and then leads into an overview of the evolution of system hardware and detector performance. The advancements in detector capabilities have opened the doors to new types of data collection and analysis. With an understanding of the benefits of the latest technology, the webinar concludes with some examples of applications, which are now possible because of these state of the art new developments.

EDAX Inc.
91 McKee Drive
Mahwah, NJ 07430
Phone (201) 529-4880
E-mail: info.edax@ametek.com
www.edax.com

Art and Layout
Jonathan McMenamin

Contributing Writers
Mike Coy
Matt Nowell
Tara Nylese
Jens Rafaelsen
Bruce Scruggs